Hidrobiológica 2010, 20 (2): 158-170

Comparative analysis of several digital methods to recognize diatoms

Análisis comparativo de varios métodos digitales para el reconocimiento de diatomeas

Josué Álvarez-Borrego[1]
and Selene Solorza[2]

[1]Centro de Investigación Científica y de Educación Superior de Ensenada, División de Física Aplicada, Departamento de Óptica, Carretera Ensenada-Tijuana, No. 3918, Fraccionamiento Zona Playitas, Ensenada, B. C., 22860 México
[2]Facultad de Ciencias, UABC, Ensenada, B. C., México.Km. 103 Carretera Tijuana-Ensenada, Ensenada, B. C., 22860
e-mail: josue@cicese.mx

Álvarez-Borrego, J. and S. Solorza. 2010 Comparative analysis of several digital methods to recognize diatoms. *Hidrobiológica* 20(2): 158-170.

ABSTRACT

In this paper, several methods are presented and compared in order to choose the best digital algorithm to recognize the diatoms species. A digital system of invariant correlation to position and rotation is constructed. Based in a binary ring mask an average signature filter for a selected image is produced in four different ways and compared with variance spectrum modified methodology using four different ways too. It is conclusive that the best methodology for this case is presented in the first method when the binary mask with a nonlinear filter is used without high frequencies enhanced in the variance spectrum of the input image using an average filter of 10 input rotated images. Moreover the confidence level for this case was 100%. The second best case was for the average filter f_{18}, with the same confidence level, but where the difference in time is more than one minute. One of the advantages of these kinds of methodologies is that an entire process can be repeated in the same way without mistakes and the diatoms images are kept save in a hard disk of the computer, so everybody can see again the diatom information of some special localization of the ocean.

Key words: Automatic identification of diatoms, image processing, invariant correlation, pattern recognition.

RESUMEN

En este artículo, se presentan y se comparan varios métodos para escoger el mejor algoritmo digital para reconocer especies de diatomeas. Se propone un sistema digital de correlación invariante a posición y rotación el cual está basado en una mascarilla binaria con cuatro diferentes caminos a seguir que produce una firma promedio para una cierta imagen seleccionada. Estos cuatro diferentes modos de correlación se comparan con una nueva metodología de espectro de varianza modificada que también utiliza cuatro maneras distintas de correlación. Es concluyente que los mejores resultados corresponden al método que utiliza la máscara binaria con una firma promedio de 10 imágenes rotadas y el uso de un filtro no lineal y sin realce del contenido de frecuencias del espectro de variancia de la imagen de entrada. El nivel de confianza para este caso fue de 100%. El segundo mejor caso, con el mismo nivel de confianza, fue para el filtro promedio de 18 imágenes rotadas, siendo la diferencia en tiempo de cómputo de más de un minuto. Una de las ventajas de esta clase de metodologías es que un proceso completo puede ser repetido de la misma manera y sin errores y además las imágenes de diatomeas pueden ser guardadas en un disco duro de

computadora de tal manera que cualquier persona pueda tener acceso a la base de datos de alguna localización especial en el océano.

Palabras clave: Identificación automática de diatomeas, procesamiento de imágenes, correlación invariante, reconocimiento de patrones.

INTRODUCTION

Microscopy is the principal method used to identify and count phytoplankton. Microscopical counts have been used to describe phytoplankton communities and their spatial and temporal distribution patterns, and have also been used to convert phytoplankton numbers to biomass or energy (e. g. in terms of organic carbon or calories, respectively) (Pech-Pacheco & Álvarez-Borrego, 1998). However, microscopical examination entails considerable time and labor for the processing of a large number of samples (Furuya, 1982); moreover, mistakes are easily made. Methods enabling the rapid identification and quantification of organisms in a phytoplankton sample are needed. Since 40 years ago, Dr. Silverio Almeida's group applied for the first time optical system in order to identify diatoms (Almeida *et al*., 1972, 1978; Cairns *et al*., 1972; Almeida and Eu, 1976; Fujii and Almeida, 1979a-b; Fujii *et al*., 1980). These studies proved the usefulness of diffraction patterns (Cairns *et al*., 1982). However, none of the studies analyze in detail the problems that are encountered during the recognition process, such as the invariance in the localization of the organisms within the image, the rotation and the different scale of the organisms, the background noise problem generated by bodies foreign to the organisms that are found in an image (detritus, inorganic particles, etc.), and the morphological variation of the species, among others, which in one way or another modify the frequencies information that form the image, generating erroneous identifications.

Circular harmonic filters have been applied to identify plankton. With this kind of filters the rotation of the organisms in the sample is solved. The advantages of these filters are numerous. First, the correlation plane is invariant to rotation, and second there are a great number of theoretical studies that have proved their sensitivity to noise (Zavala-Hamz & Álvarez-Borrego, 1997). The disadvantage is that they lose their power of discrimination if the expansion center, or proper center, is not previously selected and moreover excessive computer time is used in all the procedure.

An optical system invariant to position, rotation and scale was applied to identify five phytoplankton species of the *Ceratium* genus (family Ceratiidae) (Pech-Pacheco & Álvarez-Borrego, 1998). To recognize the organisms, they used the frequency content of the images like start point (Zavala-Hamz *et al*., 1996; Pech-Pacheco *et al*., 1999). Pech-Pacheco *et al*., (1999) could to identify *Ceratium furca* Lemmermann images with detritus, air-bubbles and with fragments of various species with a confidence level of 90%.

Small fragments of 12 species of fossil diatoms were identified with an invariant digital system to position, rotation and scale and a numerical simulation was performed in order to correlate diatom fossils species with phase-only filters (Villalobos-Flores *et al*., 2001). Each fragmented image was compared with its original image and other fragments in order to find the minimum information required for the identification of the species.

Diatoms are one of the basic sources for the formation of organic matter in the ocean, and actively participate in sedimentation, not only during recent periods of time but through the remote past. The presence of diatom valves in marine paleoenvironments has been used for the study of climatic changes as well as geomorphological process (Hajós, 1976; Koizumi & Tanimura, 1985). One of the most important features for the recognition of diatom species as paleoenvironment and paleoclimatic indicators is the high correlation between the groups of diatoms and their ecophysiological behaviour, this permit to associate the species with diverse geological and hydrodynamic features.

The identification of diatom fossils requires the analysis of a great number of valves per sample. Generally, to obtain relative abundances and diversity indexes, diatom counts must go from 400 to 10^7 structures per gram (Esparza-Álvarez, 1995). The analysis of these samples requires a great amount of time and experience and, on the other hand, the samples analyzed frequently contain material with different fragmentation degrees and this can lead to confusion and loss of information. Therefore, it is necessary the development of new techniques to facilitate the species recognition.

In this paper, several methods are presented and compared in order to choose an efficient algorithm according with the level of confidence and less computational cost to recognize the diatoms species (Figs. 1-21).

MATERIAL AND METHODS

The diatom samples are from Cuenca de San Lázaro in Baja California. This is localized to the northwest to Cabo San Lázaro to 25º 10′ N of latitude and 112º 45′ W of longitude. The Cuenca has a deep of about 540 m. These samples were taken in 1996 in an oceanographic ship called El PUMA. For specific details of the characteristics of the samples see Esparza-Álvarez, 1999.

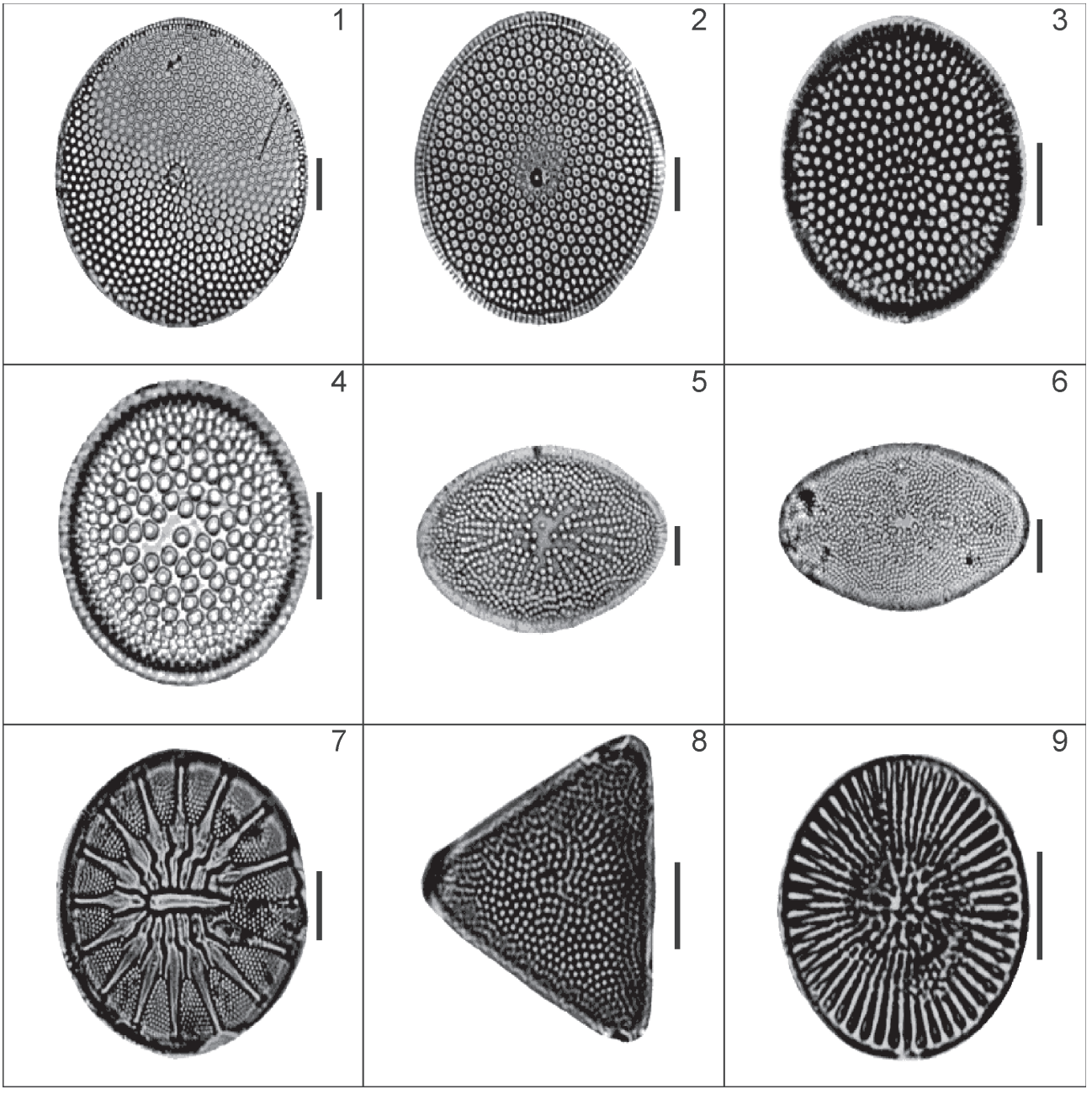

Figs. 1-9. Fig. 1. *Azpeitia nodulifera* (Schmidt) Fryxell *et* Sims, Fig. 2. *Azpeitia* sp, Fig. 3. *Coscinodiscus radiates* Ehrenberg, Fig. 4. *Actinocyclus ingens* Rattray, Fig. 5. *Actinocyclus ellipticus* Grunow in van Heurck, Fig. 6. *Actinpcyclus ellipticus* var. *moronensis* (Deby ex Rattray) Kolbe, Fig. 7. *Asteromphalus imbricatus* Wallich, Fig. 8. *Pseudotriceratium cinnamomeum* (Greville) Grunow, Fig. 9. *Stephanodiscus* sp. Figs. 4-6, 8-9 with scale bar of 10 μm. Figs. 1-2, 7 with scale bar of 20 μm. Fig. 3 with scale bar of 25 μm.

Binary ring mask. A digital system of invariant correlation to position and rotation is constructed based in a binary ring mask producing a signature filter of the selected image.

The mask of a selected image, named *I*, is built by taking the real part of its 2D-Fourier transform (FT), given by

$$f(x,y) = \mathrm{Re}(FT(I(x,y))) \quad (1)$$

where (x,y) represent a pixel of the image. Based on equation (1), we obtained the one-variable function,

$$z(x) = \begin{cases} 1, & \text{if } f(c_x,y) > 0 \\ 0, & \text{otherwise} \end{cases} \quad (2)$$

where (c_x, c_y) is the centred-pixel of *I* and y goes from 0 to wide of *I*, where *I* is an square image. Next, taking the vertical axis as the

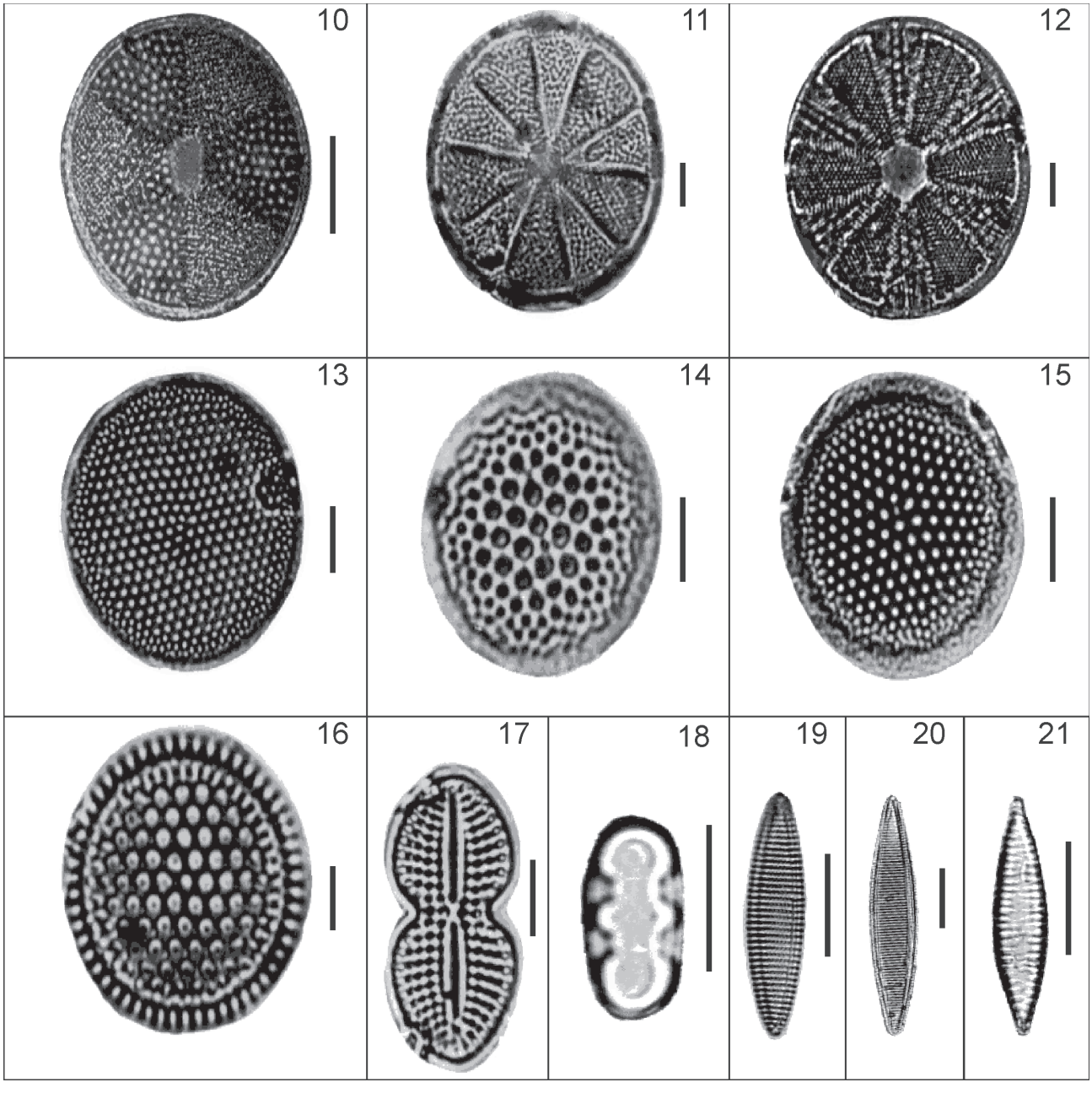

Figs. 10-21. Fig. 10. *Actinoptychus undulates* (Bailey) Ralf, Fig. 11. *Actinoptychus bipunctatus* Lohman, Fig. 12. *Actinoptychus splendens* (Shadbolt) Ralf ex Pritchard, Fig. 13. *Thalassiosira kozlovii* Makarova, Fig. 14. *Thalassiosira oestruppi* var. 1, Fig. 15. *Thalassiosira oestruppi* var. 2, Fig. 16. *Thalassiosira domifacta* (Hendey) Jouse, Fig. 17. *Diploneis bombus* Cleve-Euler in Backman *et* Cleve-Euler, Fig. 18. *Denticulopsis praedimorpha* Barron ex Akiba, Fig. 19. *Nitzchia praereinholdii* Schrader, Fig. 20. *Nitzschia reinholdii* Kanaya emend Barron *et* Baldauf, Fig. 21. *Bogorovia praepaleacea* (Schrader) Jouse. Figs. 14-15 with scale bar of 5 μm. Figs. 12-13, 16-18, 20 with scale bar of 10 μm. Figs. 10-11, 19 with scale bar of 15 μm. Fig. 21 with scale bar of 20 μm.

rotation axis, the graph of Z is rotated 360° to obtain concentric cylinders of height one, different widths and centered in (c_x, c_y). Finally, mapping those cylinders in two dimensions we built the binary ring mask associated to image *I*.

The objective is identifying a specific target (diatom to recognize) no matter the angle of rotation presented on the vertical-axis. In order to have invariance to position we did the binary mask from the frequency content of the image. So, the mask is applied in the Fourier plane for sampling the frequencies pattern of the object; Figure 22 shows two examples. In the figure 22(a) we have the target or the image to be recognized. The frequency content (Fourier domain) is obtained for each image (Fig. 22(b)).

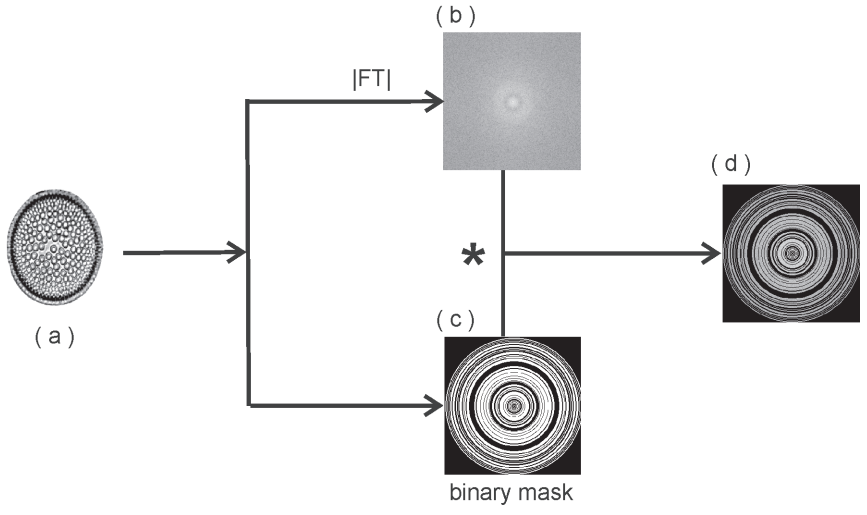

(A) *Actinocyclus ingens*

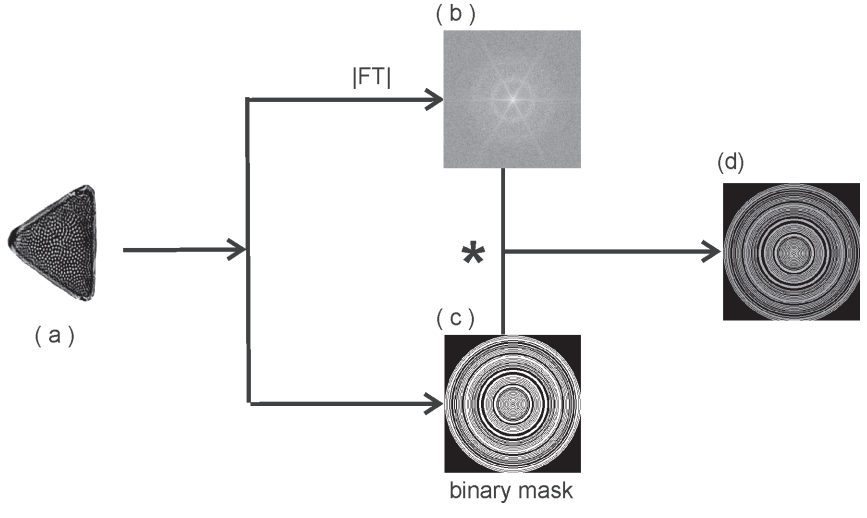

(B) *Pseudotriceratium cinnamomeum*

Figure 22. Two ring mask examples. a) the diatom image, b) the absolute value of its frequency content, c) the binary mask, d) the binary mask applied to b).

When equations 1 and 2 are applied to the frequency pattern the binary mask is calculated (Fig. 22(c)). After this, the frequency image is multiplied element by element by the binary mask obtaining the image showed in figure 22(d). For having a better visualization in the images a log was applied in figures 22(b) and 22(d). Finally, the modulus of the Fourier transform for each ring is summed and then assigned to the corresponding ring index to obtain the signature of the image. Because the signature of the image depends upon the number of rings in the mask, and the mask changes with the target, the length of the signature also change.

Figure 23 shows the procedure of the digital correlation system invariant to position and rotation. In this method, the first step selects the target. In step 2, the real value of the FT of the target is obtained. The binary mask of concentric rings is built (step 3). The images rotated are given (step 4). A parabolic mask is applied (Pech Pacheco *et al.,* 2003) or not, depending of the decision if we want to enhance the high frequencies in the filter or not (step 5). Next, the modulus of the FT of each image is obtained (step 6). When the binary mask is applied to each |FT| obtained in step 6 the signature of each image rotated is obtained (step 7) and an average filter of the target is calculated by aliasing (step 8). Figures 24 and 25 show two examples for step 8 of the procedure considering the enhancement of the high frequencies in the filter or not. In figure 24a we can see the signature when the parabolic mask was

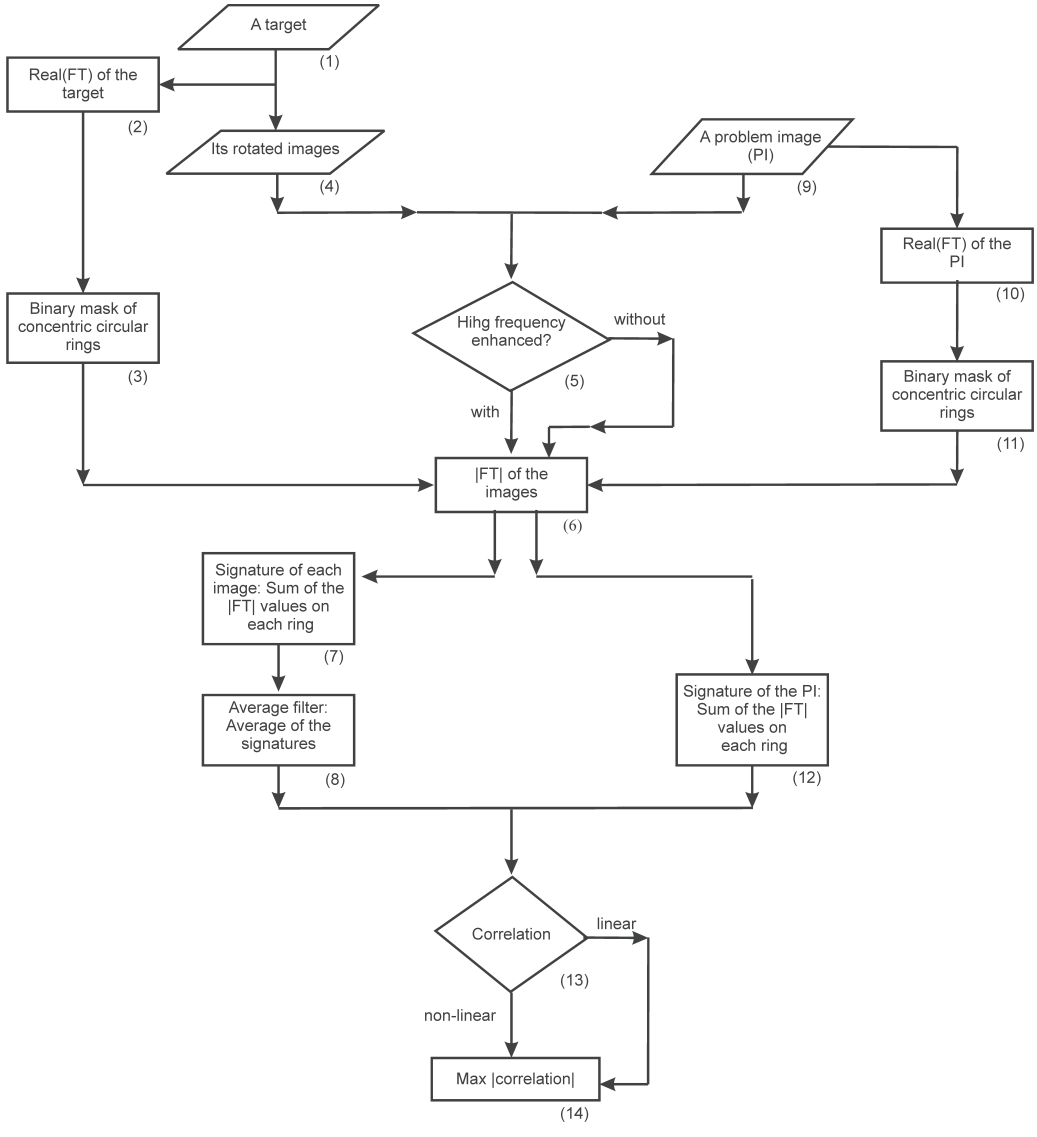

Figure 23. Binary mask methodology with its different variants.

not applied for the average signature filter of *Actinocyclus ingens* Rattray (specie A, Figs. 1-21) and figure 24b shows a comparison of the signatures of *A. ingens* and *Pseudotriceratium cinanomeum* (Greville) Grunow(specie M, Figs. 1-21). Figure 25 shows the signature filters, with the same diatoms, when the parabolic mask was applied.

For making the average signature filter of a given target, a complete rotation of 360 deg is performed to it with a rotation angle of $\Delta\theta$ deg; hence we generate $360/\Delta\theta$ images. Then, the signatures of those images are obtained to average them to build the average filter of the target, with $\Delta\theta$ = 20 deg, thus the average filter is constructed with 18 images. Here we choose the number of images in the filter making this work more flexible (Figs. 24-25).

To discriminate between images, a problem image (PI) is selected (step 9 in Fig. 23); it could be any image different or similar to the target. Then, the signature of the problem image is obtained following the steps 10, 11, 5, 6 and 12 shown in Fig. 23.

Then, in step 13 the signature of the PI is compared with the average filter *f* to recognize or not the target using a linear correlation, C_L (in this case a phase-only correlation), that is

$$C_L(PI, F) = PI \oplus f = FT^{-1}\left(FT(PI)e^{-1\phi_f}\right) \qquad (3)$$

where $\oplus$ means correlation, $i = \sqrt{-1}$ and ϕ_f is the phase of the Fourier transform of the linear filter; or we can use a non-linear correlation between them, C_{NL}, of the form (Guerrero-Moreno & Álvarez-Borrego, 2009).

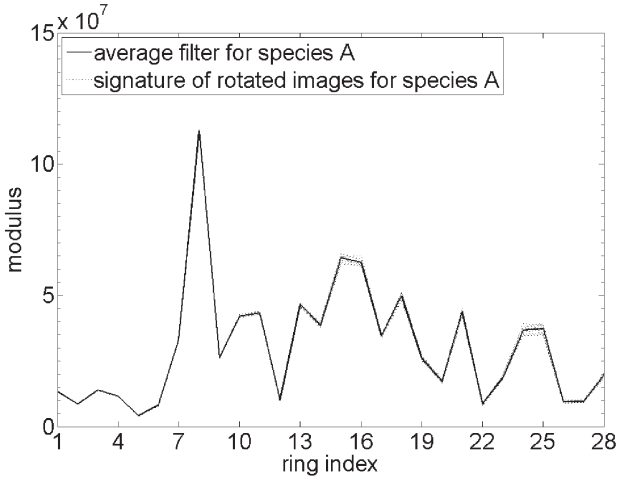

(a)

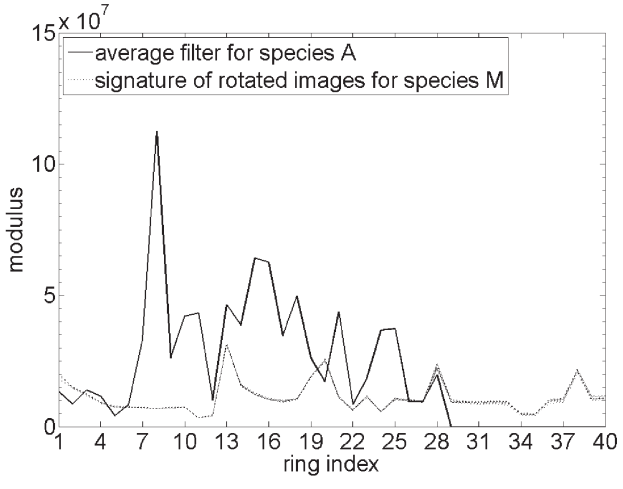

(b)

Figure 24a-b. a) Average filter for specie A without the high frequency enhanced, b) Comparison of the average filter for specie A and M without the high frequency enhanced.

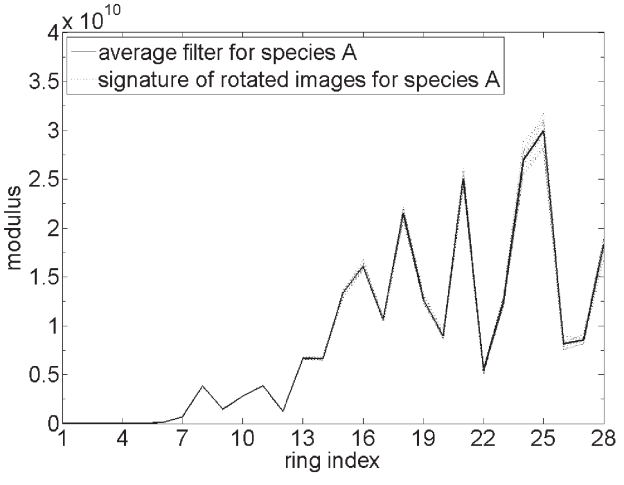

(a)

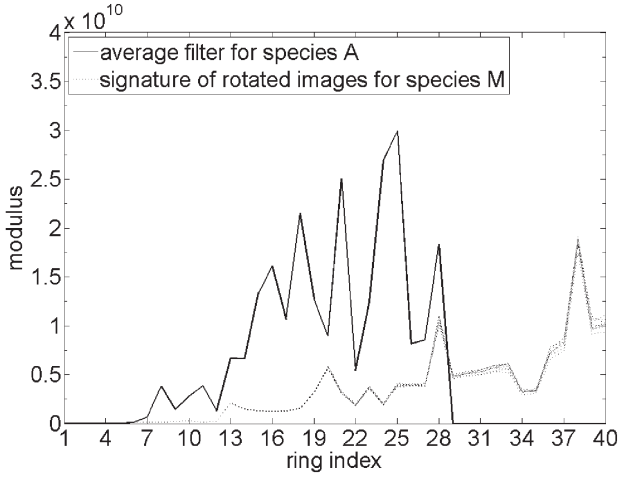

(b)

Figure 25a-b. a) Average filter for specie A with the high frequency enhanced, b) Comparison of the average filter for specie A and M with the high frequency enhanced.

$$C_{NL}(PI, f) = PI \oplus f = FT^{-1}\left(|FT(PI)|^k \, e^{i\phi_{PI}} |FT(f)|^k \, e^{-i\phi_f}\right) \quad (4)$$

with ϕ_{PI} being the phase of the Fourier transform of the PI and $0 < k < 1$ is the non-linearity factor. In this work $k = 0.1$.

To compute the correlation, the average filter and the signature of the problem image vectors need to have the same length. Because of the use of different ring masks this not happens always, hence zeros are adding to the shorter length vector to match the length of both vectors. If the maximum value of the magnitude for the correlation (step 14) is significant, hence, the problem image contains the target, otherwise has an image different to the target.

The second method used in this comparison was described by Álvarez-Borrego and Castro-Longoria, (2003). News modifications to this algorithm are presented in figure 26. The variance spectrum (square of the module of the frequency pattern of the image) is obtained (step 3) from the target (diatom to be recognized) (step 1) and from the problem image (step 2) in order to have invariance to position. A parabolic mask is applied or not to each variance spectrum depending of the decision if we want to enhance the high frequencies (step 4). In step 5, a polar mapping is obtained in order to have the invariance to rotation and again the Fourier transform is applied in order to have the frequency pattern of the target and the problem image (step 6). In step 7 we decide if we want a linear or a non-linear correlation between them. If the correlation value is significant, hence, the target is

Table 1. Binary ring mask: Diatoms confidence level (greater or equal than) for an average signature filter computed of

	Linear filter				Non-linear Filter			
	without high frequencies enhanced		with high frequencies enhanced		without high frequencies enhanced		with high frequencies enhanced	
species	f_{10}	f_{18}	f_{10}	f_{18}	f_{10}	f_{18}	f_{10}	f_{18}
A	100%	100%	100%	100%	100%	100%	100%	100%
B	100%	100%	100%	100%	100%	100%	100%	100%
C	100%	100%	95.4%	95.4%	100%	100%	100%	100%
D	100%	100%	100%	100%	100%	100%	100%	100%
E	95.4%	95.4%	100%	100%	100%	100%	100%	100%
F	100%	100%	100%	100%	100%	100%	100%	100%
G	100%	100%	95.4%	95.4%	100%	100%	100%	100%
H	100%	100%	100%	100%	100%	100%	100%	100%
I	100%	100%	100%	100%	100%	100%	100%	100%
J	100%	100%	100%	100%	100%	100%	100%	100%
K	100%	100%	100%	100%	100%	100%	100%	100%
L	100%	100%	100%	100%	100%	100%	100%	100%
M	95.4%	95.4%	95.4%	95.4%	100%	100%	100%	100%
N	100%	100%	100%	100%	100%	100%	100%	100%
O	100%	100%	100%	100%	100%	100%	100%	100%
P	100%	100%	100%	100%	100%	100%	100%	100%
Q	100%	100%	100%	100%	100%	100%	100%	100%
R	100%	100%	100%	100%	100%	100%	100%	100%
S	100%	100%	100%	100% without C	100%	100%	100%	100%
T	100%	100%	100%	100%	100%	100%	100%	100%
U	100%	100%	68.3%	68.3%	100%	100%	100%	100%
Time per correlation (secs)	0.125491	0.125604	0.126209	0.126366	0.126203	0.126360	0.126732	0.127040
Time for 158,760 correlations*	5hrs 32' 3" = 19,923"	5hrs 32' 21" = 19,941"	5hrs 33' 57" = 20,037"	5hrs 34' 22" = 20,062"	5hrs 33' 56" = 20,036"	5hrs 34' 21" = 20,061"	5hrs 35' 20" = 20,120"	5hrs 36' 09" = 20,169"

* Correlations for the 7560 different images.

recognized in the problem image (step 8), otherwise has an image different to the target.

Figures 27 and 28 show two examples when the variance spectrum methodology is applied to *Actinocyclus ingens* (specie A, Figs. 1-21) and *Pseudotriceratium cinanomeum* (specie M, Figs. 1-21). The spectrum variance with high frequencies enhanced is log visualized in figures 27a and 28a, respectively, for these two species and the spectrum variance without high frequencies enhanced is log visualized in figures 27d and 28d, respectively. The output correlations in log visualized are shown in figures 27b, 27c, 27e, 27f, 28b, 28c, 28e and 28f. These last figures mentioned show the different ways can be taken in order to recognize or not an organism in the problem image. Each way does a different algorithm with different computer time in the process.

RESULTS

The algorithms were programming in Matlab 7.1 in a MacBook Pro3,1 with a Intel Core 2 Duo processor of 2.4 GHz, memory of 2 GB 667 MHz DDR2 SDRAM, L2 Cache of 4 MB and 800 MHz of Bus Speed.

Table 1 and 2 give us a review of the results when we did the correlation of all the 21 species (Figs. 1-21), each one versus all of them and its 360 rotated images. First, in Table 1, we have

Table 2. Spectrum filter: Diatoms confidence level (greater or equal than) for an average signature filter computed of

	Linear filter				Non-linear filter			
	without high frequencies enhanced		with high frequencies enhanced		without high frequencies enhanced		with high frequencies enhanced	
species	f_{10}	f_{18}	f_{10}	f_{18}	f_{10}	f_{18}	f_{10}	f_{18}
A	100%	100%	100%	100%	100%	100%	95.4%	95.4%
B	100%	100%	100%	100%	100%	100%	95.4%	95.4%
C	100%	100%	100%	100%	100%	100%	100%	100%
D	95.4%	95.4%	100%	100%	100% without A	100% without A	68.3% without K, N	68.3% without N
E	100%	100%	100%	100%	95.4%	95.4%	68.3% without D	68.3% without D
F	100%	100%	100%	100%	100%	100%	95.4% without E	95.4% without E
G	100%	100%	100%	100%	100%	100%	68.3%	68.3%
H	100%	100%	100% without U	100% without U	100% without U	100% without U	68.3%	95.4% without P
I	100%	100%	100%	100%	100%	100%	68.3% without S	95.4% without N
J	100%	100%	95.4%	95.4%	100%	100%	68.3% without O	68.3%
K	100%	100%	95.4%	95.4%	100%	100%	68.3% without A, R	95.4% without J
L	100%	100%	100%	100%	100%	100%	68.3%	95.4% without O
M	100%	100%	100%	100%	95.4%	95.4%	95.4% without S	95.4% without S
N	68.3%	68.3%	95.4%	95.4%	100%	100%	95.4% without R	68.3% without R
O	100%	100%	100%	100%	100% without K	100% without K	68.3%	95.4% without B
P	95.4%	68.3%	100%	100%	68.3%	95.4% without D	95.4%	68.3%
Q	100%	100%	95.4%	95.4%	95.4%	100%	95.4% without B, C	95.4% without B, C
R	100%	100%	95.4%	95.4%	100%	100%	68.3% without L, T	68.3% without L, T
S	100%	100%	95.4%	95.4%	100%	100%	95.4% without J, R	95.4% without J, R
T	100%	100%	95.4%	95.4%	100% without L	100% without L	68.3% without A	95.4% without A, Q
U	100%	100%	68.3%	68.3%	100% without H	100% without H	68.3%	95.4%
Time per correlation (secs)	2.472871	2.473563	2.475428	2.475491	2.576688	2.587540	2.593965	2.601341
Time for 158,760 correlations*	4d 13hrs 03' 13" = 392593"	4d 13hrs 05' 03" = 392703"	4d 13hrs 09' 59" = 392999"	4d 13hrs 10' 09" = 393009"	4d 17hrs 37' 55" = 409075"	4d 18hrs 06' 38" = 410798"	4d 18hrs 23' 38" = 411818"	4d 18hrs 43' 09" = 412989"

* Correlations for the 7560 different images.

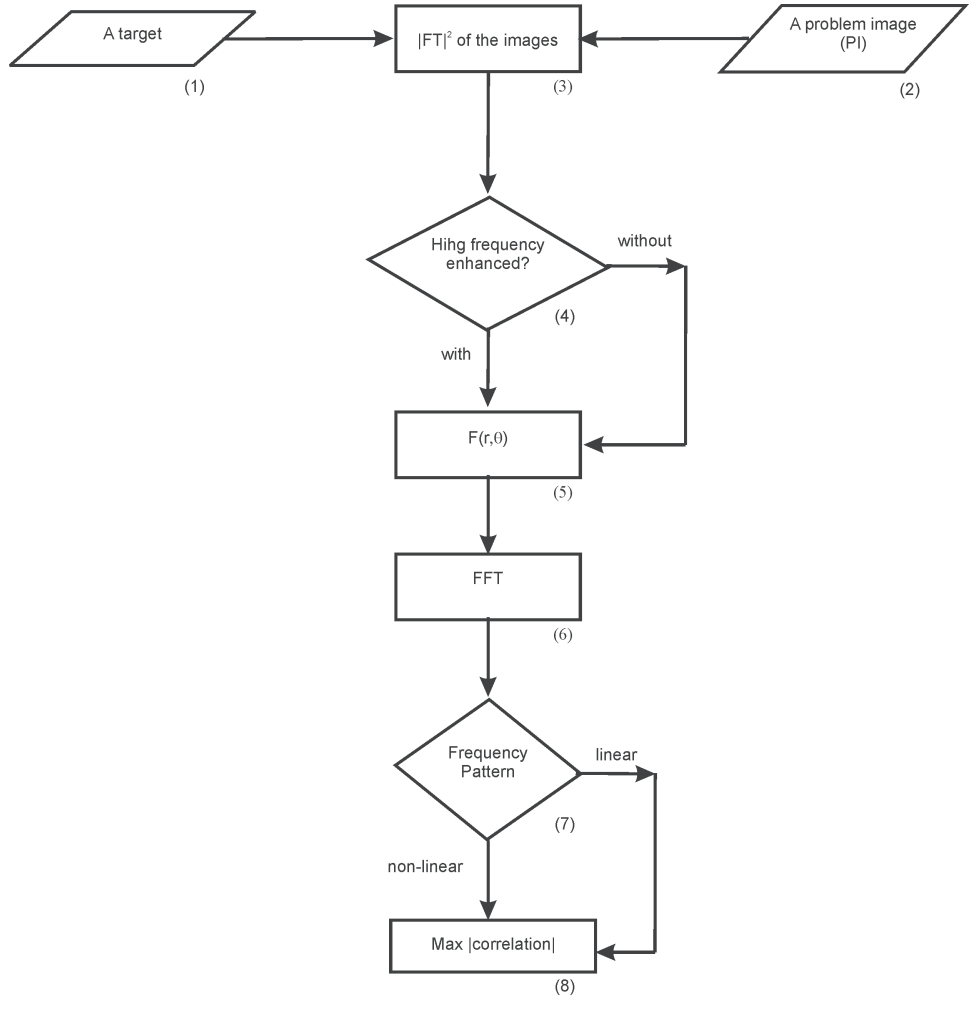

Figure 26. Spectrum filter methodology with its different variants.

the result for the linear and nonlinear filters using the binary ring mask (Fig. 23), without and with high frequencies enhanced for two kinds of average filters: f_{10} and f_{18} (Solorza & Álvarez-Borrego, 2010). The sub index number indicates the number of images used in the average filter. In the first column of the Table 1 we have the type of the species used according with Figs. 1-21.

We can see in Table 1, when the binary mask methodology uses the linear filter without high frequencies enhanced in the variance spectrum, the discrimination was at least of a level of confidence of 95.4% for species E and M when the filters f_{10} and f_{18} were used. For the other species the confidence level was 100%.

Using the linear filter with high frequencies enhanced in the variance spectrum the results are not better. For example using the filter f_{10} the discrimination was at least of a level of confidence of 95.4% for species C, G and M and at least of a level of confidence of 68.3% for specie U. For the other species the level of confidence was of 100%. When the filter f_{18} was used a 95.4% was obtained for species C, G and M. A 68.3% of level of confidence for species U was obtained. The rest had a 100% of confidence level in the recognition of the species except the specie S which is not considering the specie C.

We can see in Table 1 t when we used the linear filter the best computer time was for the filter f_{10} without and with high frequencies enhanced, the filter f_{10} had a better performance in both cases.

The results obtained with the nonlinear filter using the binary ring mask (Fig. 23), can be seen in the last four columns. For all the cases, without or with high frequencies enhanced, the confidence level was of 100%. In other words, all the species could be recognized without mistakes. The best time computer for this case is for the nonlinear filter without high frequencies enhanced in the variance spectrum being of 0.126203 secs per correlation and using the average filter f_{10}.

For the second algorithm and all its variants (Fig. 26) the results are presented in Table 2. Again, the first column shows the species to be studied in according with Figs. 1-21. The first four columns show the results for the linear filter without or with high

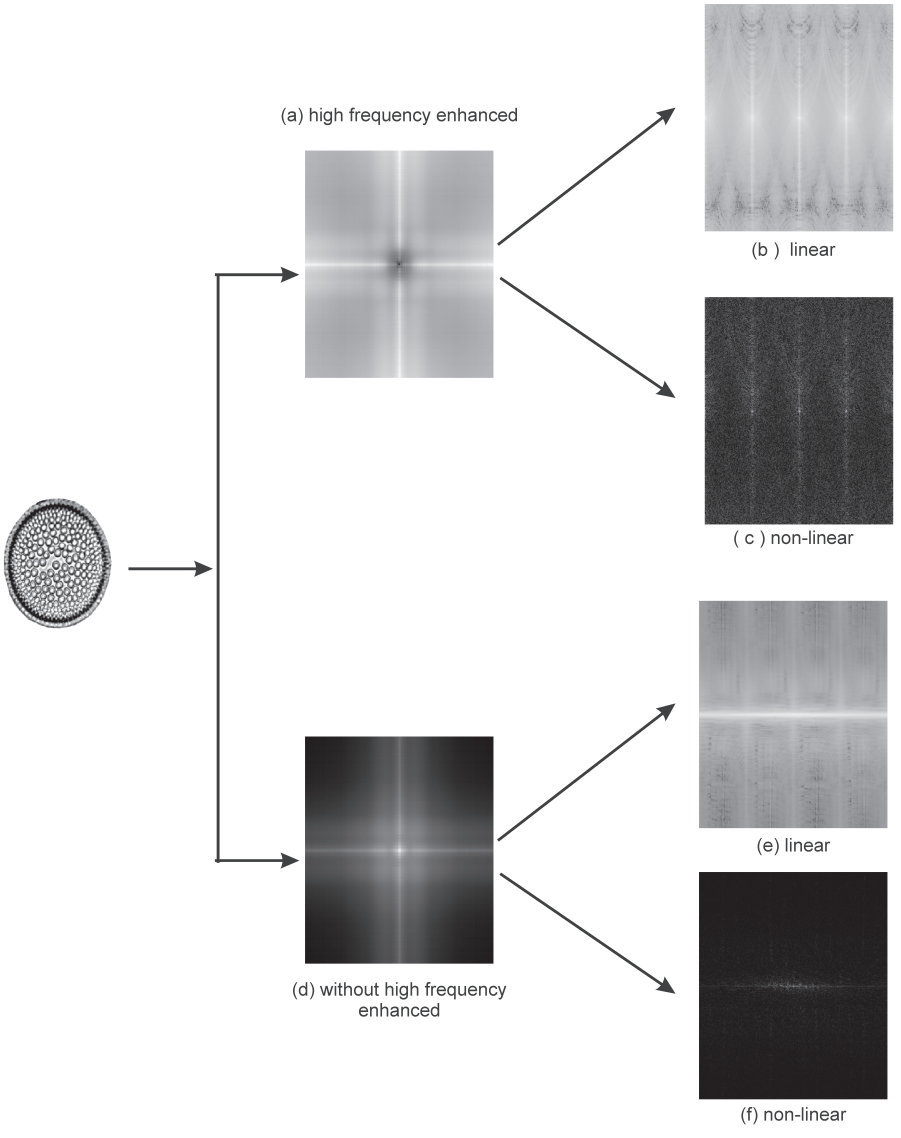

Figure 27. Methodology of the figure 26 applied to species A showing the differents variants in the process.

frequencies enhanced of the variance spectrum for the average filters f_{10} and f_{18}. The worst scenario for the filter f_{10} is for the specie N with 68.3% of confidence level following the species D and P with 95.4% of confidence level. The other cases showed a 100% of confidence level in the recognition of the species. For the filter f_{18} the worst scenario is for the case N and P following the case D with 95.4% of confidence level. The other cases showed a 100% of confidence level in the recognition of the species. When the average linear filter, f_{10}, is used with high frequencies enhanced seven cases presented 95.4% of confidence level only: J, K, N, Q, R, S and T. The worst scenarios were the cases H and U. The other cases showed 100% of confidence level. For the average linear filter f_{18} the same result was found.

Showing the results of the last four columns of the Table 2 we see a bad scenario for both of the cases without or with high frequencies enhanced and for both of the filters f_{10} and f_{18}. In several of the cases many of the species could not be recognized with this kind of methodology. The worst case was the average nonlinear filter, f_{18}, with high frequencies enhanced with 14 cases. f_{10} presented 12 bad cases.

However, for all the cases in this Table 2 the computer time is about four days and several hours in order to obtain the results in this species recognition methodology.

DISCUSSION

In this paper several methods are presented and compared in order to choose the best digital algorithm to recognize the diatoms species (Figs. 1-21). We will choose the algorithm with more level of confidence and less computational cost. We used f_{10} and

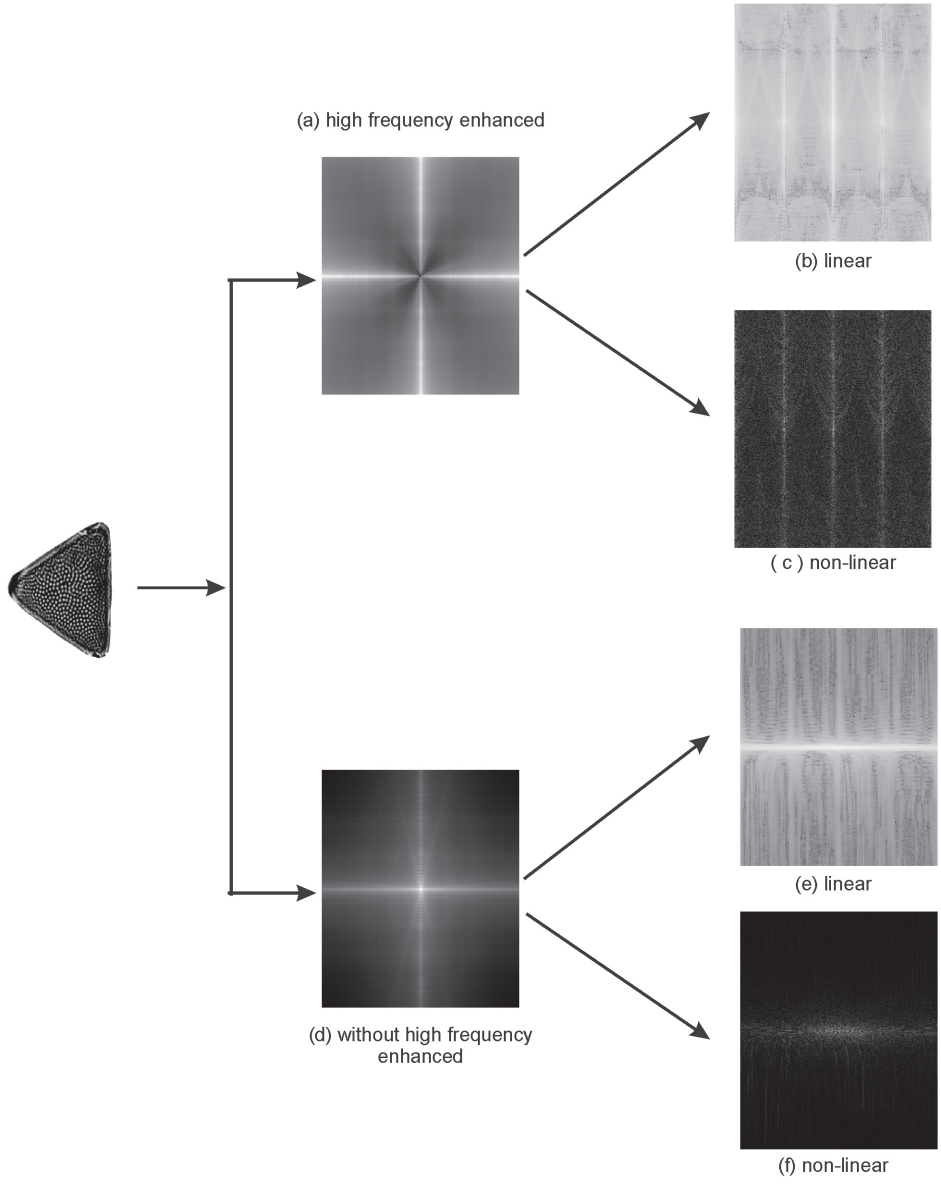

Figure 28. Methodology of the figure 26 applied to species M showing the differents variants in the process.

f_{18} average filters because it was shown that these filters have a very good performance, being f_{10} better than f_{18} (Solorza & Álvarez-Borrego, 2010).

Each filter f_{10} and f_{18} of each species was correlated with the 360 images rotated of each species, $\Delta\theta = 1$ deg. In other words, we worked with 7560 images (21 times 360) in each correlation. Considering this number of images, the computer time used in the first method (Fig. 23) with the nonlinear filter without high frequencies enhanced was so short. Moreover the confidence level for this case was 100%. The second best time was for the average filter f_{18} where the difference is less than one minute.

One of the advantages of these kinds of methodologies is that an entire process can be repeated in the same way without mistakes and the diatoms images are kept save in a hard disk of the computer, so everybody can see again the diatom information of some special localization of the ocean.

Taking account all the works in the past about to identify automatically zooplankton, the methodology presented in the Fig. 23 is faster and has the best level of confidence.

The second methodology with all its variants (Fig. 26) did not have a good performance when the diatoms images were analyzed; however it had a very good performance when copepods were studied (Álvarez-Borrego & Castro-Longoria, 2003) using a

linear filter with the high frequencies enhanced of the variance spectrum.

With those results we see that each particular problem has its own particular solution, however the idea is try to find a more wide application to each particular algorithm.

The novel of the algorithm presented in this paper is the introduction of the nonlinear filter associated with the binary ring mask and the use of average one-dimensional signature. This algorithm permits 100% of confidence in the recognition of the diatoms and a record time consuming in all the procedure.

ACKNOWLEDGEMENT

This document is based on work partially supported by CONACyT with grant No. 102007.

REFERENCES

Almeida, S. P., D. Del Balzo, J. Jr. Cairns, K. Dickson & G.Lanza. 1972. Holographic microscopy of diatoms. *Transactions Kansas Academic Science* 74: 257-260.

Almeida, S. P., & J. K. T. Eu. 1976. Water pollution monitoring using matched spatial filters. *Applied Optics* 15 (2): 510-515.

Almeida, S. P., S. K. Case, J. M. Fournier, H. Fujii, J. Jr. Cairns, K. L. Dickson & P. Pryfogle. 1978. Analysis of algae samples using coherent optical processing. *In:* Proceedings of ICO-II Conference. Madrid, Spain. pp. 351-354.

Álvarez-Borrego, J. & E. Castro-Longoria. 2003. Discrimination between Acartia (Copepoda: Calanoida) species using their diffraction pattern in a position, rotation invariant digital correlation *Journal of Plankton Research* 25 (2): 229-233.

Cairns, J. Jr., K. L. Dickson, G. R. Lanza, S. P. Almeida & D. Del Balzo. 1972. Coherent optical spatial filter of diatoms in water pollution monitoring. *Archives of Microbiology* 83: 141-146.

Cairns, J. Jr., S. P. Almeida & H. Fujii. 1982. Automated identification of diatoms. *Bioscience* 32 (2): 98-102.

Esparza-Álvarez, M. A. 1995. *Paleocología de sedimentos diatomaceos de la formación Tortugas en el área de Bahía Asunción, Baja California Sur, México.* Tesis Licenciatura. Facultad de Ciencias Marinas, Ensenada, B. C. México, 89 p.

Esparza-Álvarez, M. A. 1999. Variabilidad de la comunidad de diatomeas en los sedimentos de la Cuenca de San Lázaro, Baja California Sur, México. Tesis de maestría. Cicese, Ensenada, B. C. México, 113 p.

Fujii H. & S. P. Almeida. 1979a. Partially matched spatial filtering with simulated input. Society Photo-Optical Instrumentation Engineers. 177 p.

Fujii, H. & S. P. Almeida. 1979b. Coherent spatial filtering with simulated input. *Applied Optics* 18 (10): 1659-1662.

Fujii, H., S. P. Almeida & J. E. Dowling. 1980. Rotational matched spatial filter for biological pattern recognition. *Applied Optics* 19 (7): 1190-1193.

Furuya, K. 1982. Measurement of phytoplankton standing stock using an image analyzer system *Bull Plankton Soc Japan* 29: 131-132.

Guerrero-Moreno, R. E. & J. Álvarez-Borrego. 2009. Nonlinear composite filter performance. *Optical Engineering* 48 067201.

Hajós, M. 1976. Upper eocene and lower oligocene diatomaceae, archaemonadaceae and silicoflagellates in southwestern pacific sediments. *DSSP, leg 29. Initial reports DSPP.* 5 (35): 817-883.

Koizumi, I. & Y. Tanimura. 1985. Neogene diatom biostratigraphy of the middle latitude western North Pacific, Deep Sea Drilling Project Leg 86. In, Heath, G. R. Burckle, L. H. eds, Initial Report DSDP, vol. 86, pp. 269-300. U.S. Govt. Print. Office, Washington, D. C.

Pech-Pacheco, J. L. & J. Álvarez-Borrego. 1998. Optical-digital processing applied to the identification of five phytoplankton species. *Marine Biology* 132 (3): 357-365.

Pech-Pacheco, J. L., J. Álvarez-Borrego, E. Orellana-Cepeda & R. Cortés-Altamirano. 1999. Diffraction patterns applicability in identification of Ceratium species. Journal of Plankton Research 21 (8): 1455-1474.

Pech-Pacheco, J. L., J. Álvarez-Borrego, G. Cristóbal & M. Keith. 2003. Automatic object identification irrespective to geometric changes. *Optical Engineering* 42 (2): 551-559.

Solorza, S. & J. Álvarez-Borrego. 2010. Digital System of Invariant Correlation to Position and Rotation. *Optics Communication.* 283 (19): 3613-3630.

Villalobos-Flores, C. E., J. Álvarez-Borrego, J. L. Pech-Pacheco, G. Cristóbal & E. Castro-Longoria. 2001. Study of fragmented fossil diatoms using an invariant correlation method**.** *In:* Vera L.B., S.A. Ledesma & M.C. Marconi (Eds.). Proceedings 4th Iberoamerican Meeting of Optics and 7th Latin American Meeting on Optics, Lasers, and their Applications, SPIE 4419, pp. 18-21.

Zavala-Hamz, V. A., J. Álvarez-Borrego & A. Trujillo-Ortiz. 1996. Diffraction patterns as a tool to recognize copepods *Journal of Plankton Research*, 18 (8): 1471-1484.

Zavala-Hamz, V. A. & J. Álvarez-Borrego. 1997. CH filters for the recognition of marine microorganisms *Applied Optics* 36 (2): 484-489.

Recibido: 4 de diciembre de 2009.

Aceptado: 22 de julio de 2010.